

01 Jan 2022

Identifying Sources of Conducted Emissions by Measuring the Coherence Function

Xin Yan

Fuwei Ma

Wei Zhang

Kaustav Ghosh

et. al. For a complete list of authors, see https://scholarsmine.mst.edu/ele_comeng_facwork/4690

Follow this and additional works at: https://scholarsmine.mst.edu/ele_comeng_facwork



Part of the [Electrical and Computer Engineering Commons](#)

Recommended Citation

X. Yan et al., "Identifying Sources of Conducted Emissions by Measuring the Coherence Function," *2022 IEEE International Symposium on Electromagnetic Compatibility and Signal/Power Integrity, EMCSI 2022*, pp. 321 - 325, Institute of Electrical and Electronics Engineers, Jan 2022.

The definitive version is available at <https://doi.org/10.1109/EMCSI39492.2022.9889585>

This Article - Conference proceedings is brought to you for free and open access by Scholars' Mine. It has been accepted for inclusion in Electrical and Computer Engineering Faculty Research & Creative Works by an authorized administrator of Scholars' Mine. This work is protected by U. S. Copyright Law. Unauthorized use including reproduction for redistribution requires the permission of the copyright holder. For more information, please contact scholarsmine@mst.edu.

Identifying Sources of Conducted Emissions by Measuring the Coherence Function

Xin Yan^{*1}, Fuwei Ma^{*2}, Wei Zhang^{*3}, Kaustav Ghosh^{#4}, Sameer Walunj^{#5}, Philippe Sochoux^{#6}, and Victor Khilkevich^{*7}

^{*}EMC Laboratory

Missouri University of Science and Technology

Rolla, MO, USA

⁷ khilkevichv@mst.edu

[#]Juniper Networks

Sunnyvale, CA, USA

⁶ psochoux@juniper.net

Abstract—Conducted emissions (CE) is one of the electromagnetic interference (EMI) issues that pose serious compliance problems for electronic devices. For a system with several sources, estimating the contribution of each source to conducted emission at different frequencies can be a challenge. In this article, a coherence function-based signal separation method is presented and validated on two commercial power supply units (PSU). The noise generated by the PSU and measured at the line impedance stabilization network (LISN) port contains two predominantly uncorrelated signals associated with the power factor correction (PFC) and H-bridge/rectifier circuits with unknown contributions at different frequencies. Two reference signals are obtained by probing the emission signals close to the sources. By calculating the coherence between the LISN noise signal and the reference signals, the contributions of these two signals to the noise are obtained. The measurement of the signal contributions can help engineers identify the dominant sources and mitigate the emissions more efficiently over a wide range of frequencies.

Keywords—Conducted emission, coherence function, power supply unit

I. INTRODUCTION

Conducted emissions (CE) is one of the EMI problems, which brings serious compliance issues to the electronic devices. Conducted noise generated by electronic devices can be transferred to another device through parasitic capacitance, PCB traces, power/ground planes, or cables. Noise coupled to AC cables can affect the operation of other devices and can lead to malfunctions. Therefore, it is necessary to analyze and mitigate the conducted emissions. Many researchers have addressed modeling, simulation and suppression methods for different electrical devices. In [1], a conducted emission model was constructed for a switch-mode power supply by extracting the total voltage source, characterizing the coupling path, and then combining them in a circuit model. The conducted emission mechanism and EMI suppression designs of a DC/DC semi-isolated switched mode power supply is presented in [2]. In [3], modelling and simulation methodologies of conducted emission for electronic control module are demonstrated. In [4], the effect of chassis grounding and π -filters on conducted emissions are investigated. A design of an AC voltage probe for conducted emission measurement was introduced in [5], and in [6], an in-circuit conducted emissions measurement approach without a line impedance stabilization network (LISN) is addressed by extracting the common mode and differential mode impedances.

Despite the extensive research on conducted emissions, for a system that has multiple emission sources, estimating the contribution of each source at different frequencies is still a challenge. The broadband spectrum of conducted emissions contains contributions of all sources, making it difficult to analyze and identify the root cause of EMI through simulation and measurement. In this paper, a signal separation method based on coherence function for conducted emissions is proposed. The method aims to separate multiple uncorrelated inputs (e.g., emission source signals) from the outputs (e.g., conducted emissions) in a linear system, as shown in Fig. 1. This method was validated on two commercial power supply units (PSUs). Based on the proposed method, the contributions of different sources are obtained at different frequencies successfully.

The paper is organized as follows. In Section II, the coherence function and the proposed signal separation method are introduced. Section III presents the details of measurement validations on two PSUs. Section IV presents the conclusion.

II. SIGNAL SEPARATION METHOD

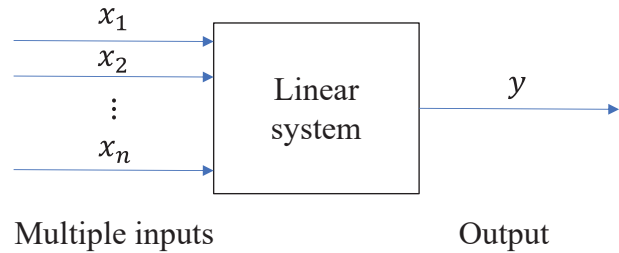


Fig. 1. Schematic of the system with multiple inputs and one output.

A. Coherence function

The coherence function between two signals x and y is defined as [7]:

$$\gamma_{xy}(f) = \frac{|G_{xy}(f)|^2}{G_{xx}(f)G_{yy}(f)}, \quad (1)$$

where the $G_{xx}(f)$ is the power spectral density of signal x , $G_{yy}(f)$ is the power spectral density of signal y , $G_{xy}(f)$ is the cross power spectral density, and $\gamma_{xy}(f)$ is the coherence between x and y . The coherence function takes values from 0 for totally uncorrelated signals to 1 for completely correlated signals. The spectral densities are the time limits of the expected values of the squared spectra of the signals, which are defined by (2) and (3):

$$G_{xx}(f) = \lim_{T \rightarrow \infty} \frac{1}{T} \langle X(t, f) X^*(t, f) \rangle, \quad (2)$$

$$G_{xy}(f) = \lim_{T \rightarrow \infty} \frac{1}{T} \langle X(t, f) Y^*(t, f) \rangle, \quad (3)$$

where X is the spectrum of signal x , Y is the spectrum of signal y , T is the observation time, $\langle \cdot \rangle$ is the averaging operator, and the asterisk denotes complex conjugate.

Considering a linear system with input x and output y , as shown in Fig. 2, the coherence between the input and output signals $\gamma_{xy}(f)$ in this case will be equal to 1 (on practice $\gamma_{xy}(f)$ is always less than 1, because of the measurement noise). However, if additional inputs to the system (besides x) are present (as in Fig. 1), the coherence between x and y will have a meaning of the fractional power of the output y that is caused by the input x . In this case the power contribution of the input x to output y could be calculated as:

$$S_{xy} = G_{yy} \gamma_{xy}. \quad (4)$$

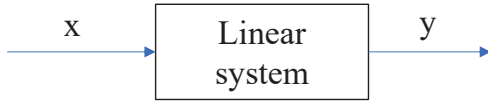


Fig. 2. A linear system that has input x and output y .

A useful property of the coherence function is that the coherence does not change due to the scaling of the input x . Assuming the scaling factor is a , and the scaled input is x' , then:

$$x' = ax \quad (5)$$

$$\gamma_{x'y}(f) = \frac{|aG_{xy}(f)|^2}{a^2G_{xx}(f)G_{yy}(f)} = \gamma_{xy}(f) \quad (6)$$

$$S_{xy} = G_{yy} \gamma_{xy} = G_{yy} \gamma_{x'y} \quad (7)$$

Therefore, for a linear system with multiple inputs, the power contributions of the inputs to the output could be calculated from the coherence functions even if the inputs signals are not directly available, but instead are measured with unknown scaling factors, for example by probes.

B. Signal Separation Method

Based on the coherence function and its properties, a signal separation method is proposed to identify the sources of the conducted emissions. Consider two uncorrelated source signals, x_1 and x_2 , and the mixed signal v defined as a linear combination of the signals:

$$v = ax_1 + bx_2 + n(t), \quad (8)$$

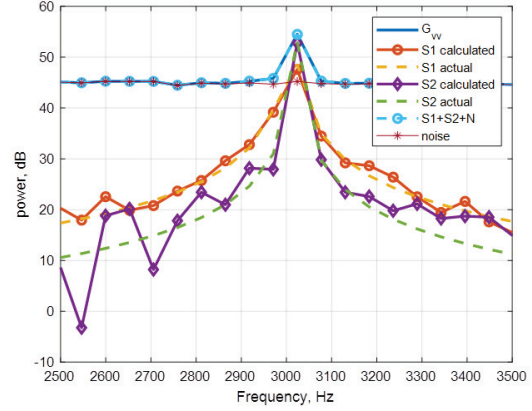


Fig. 3. An example of the signal separation.

where a is the contribution of signal x_1 , b is the contribution of signal x_2 , and $n(t)$ is the additive noise. To obtain the contributions of signals x_1 and x_2 , the reference signals r_1 and r_2 , as scaled x_1 and x_2 , are measured separately:

$$r_1 = cx_1 \quad (9)$$

$$r_2 = dx_2 \quad (10)$$

where c and d are the scaling factors (unknown in general) of the signal x_1 and x_2 respectively. The power contributions of the signals could be calculated therefore as:

$$S_1 = G_{vv} \gamma_{vr1} \quad (11)$$

$$S_2 = G_{vv} \gamma_{vr2} \quad (12)$$

A numerical example of signal separation is shown in Fig. 3. Signal 1 and signal 2 are uncorrelated sinusoidal signals (i.e. having different frequencies). The frequencies are close such that the difference between them is smaller than the spectral resolution (determined by the length of the time record) and the signals cannot be discriminated in the frequency domain (the power spectral density G_{vv} has only one peak). The mixed signal v is a sum of signal 1, signal 2, and white gaussian noise (the signal-to-noise ratio is 10 dB at the peak frequency of 3.02 kHz). By calculating the coherence functions between the mixed signal and the scaled references according to (1-3), the power densities of the contributions of signals 1 and 2 are reconstructed successfully and are very close to the actual densities. Moreover, the summation of calculated contributions and noise power density overlap with the actual power density G_{vv} of the mixed signal v .

The signal separation method has limitations. To separate the signals successfully, good signal-to-noise ratios of mixed signal and reference signals are required, and the leakage between the reference channels (i.e. coupling of the signal 1 to the reference 2 and vice versa) need to be small. In addition to this, the spectral density is obtained within a limited time as opposed to the infinite time in (2-3), leading to errors in the power spectral density estimation. These factors may affect the accuracy of the calculated power densities and contributions and deserve an additional investigation.

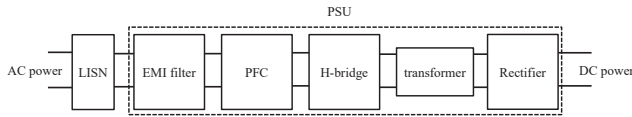


Fig. 4. Diagram of the DUT.

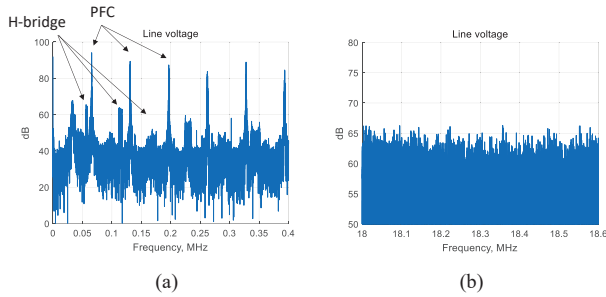


Fig. 5. Conducted emissions: (a) low frequencies, (b) high frequencies.

III. MEASUREMENT VALIDATION

A. Device Under Test

To validate the proposed signal separation method, two commercial PSUs which convert AC power to DC power are tested. The rated power of the first PSU is 900 W, and the second PSU is 1600W. In these two PSUs, power factor correction

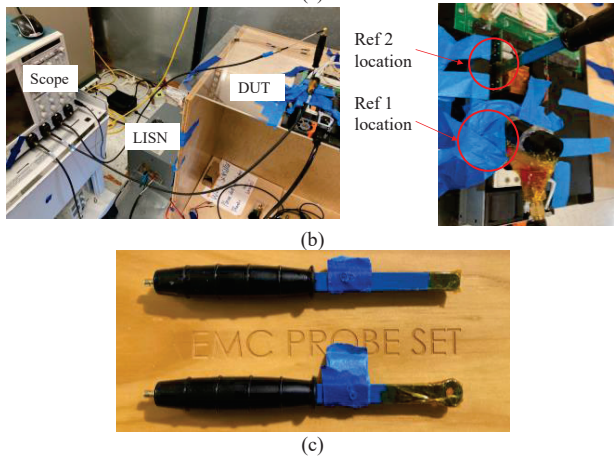
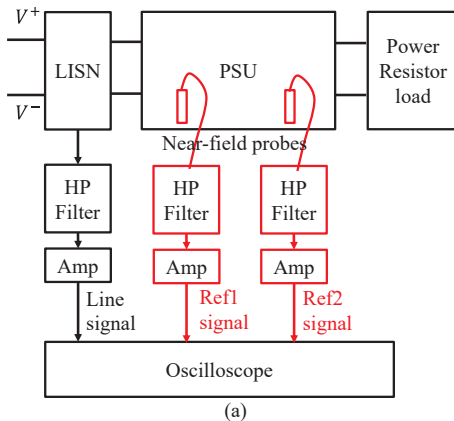


Fig. 6. (a) Diagram of the measurement setup. (b) Photos of the measurement setup. (c) Near-field probes.

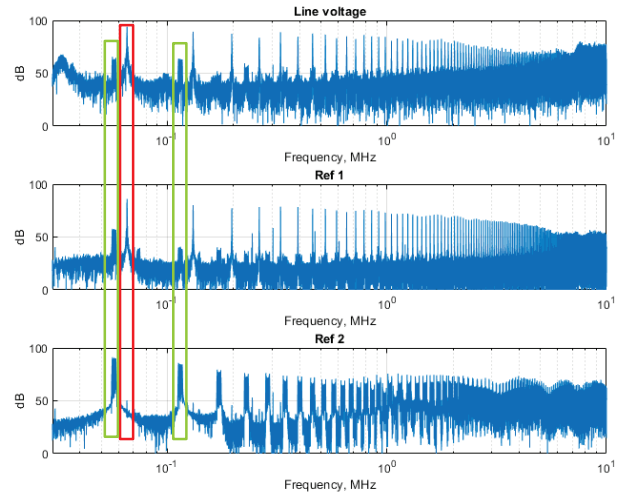


Fig. 7. Spectra of three channels at low frequencies for the 920W PSU.

(PFC) and H-bridge circuits driven by different switching sources are the main emission sources. The conducted emission is measured from the line port of the LISN. The diagram of the device under test (DUT) is shown in Fig. 4. At low frequencies the signals can be separated in the frequency domain directly, as shown in Fig. 5(a), because the harmonics of the switching signals are easily identifiable. However, at higher frequencies the spectra of the harmonics start to overlap, the total spectrum becomes continuous, and the individual signals cannot be separated in the frequency domain (Fig 5(b)). Therefore, the signal separation procedure is needed to identify the contributions of different sources.

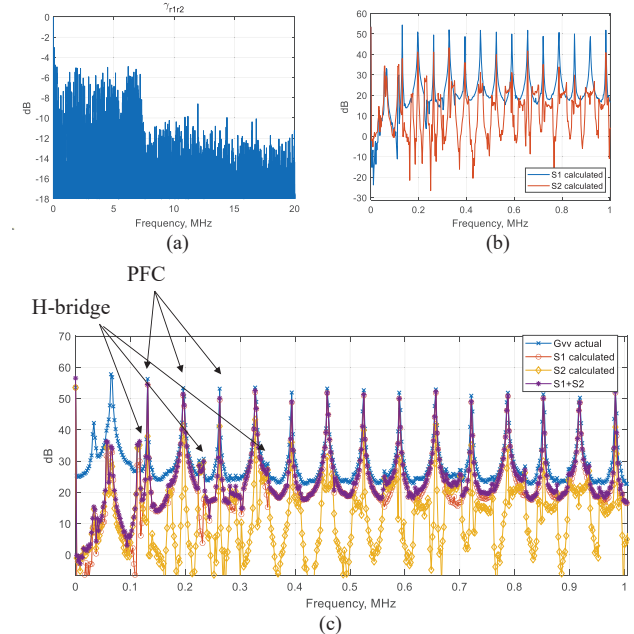


Fig. 8. Measurement Results at low frequencies for the 920W PSU. (a) coherence between reference 1 and 2. (b) Calculated contributions of signal 1 and 2 at low frequencies. (c) Comparison between the power density of line signal and summation of the contributions.

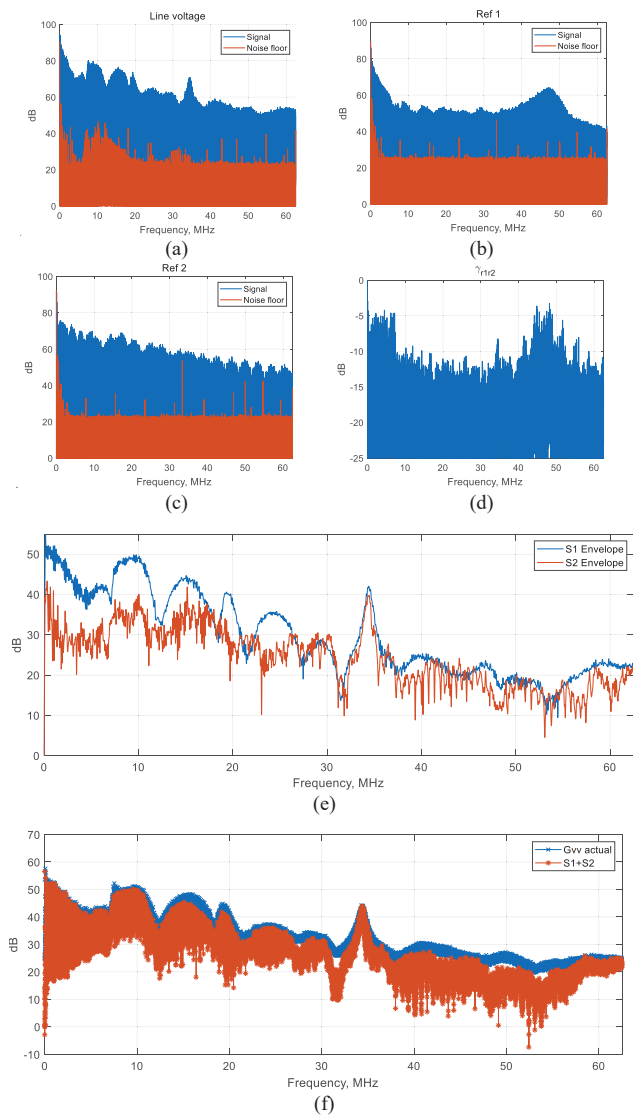


Fig. 9. Measurement results at 125 MS/s for the 920W PSU. (a) Line signal vs. noise floor. (b) Reference 1 vs. noise floor. (c) Reference 2 vs. noise floor. (d) Coherence between reference 1 and 2. (e) Calculated contribution envelopes of signal 1 and 2. (f) Comparison between the power density of line signal and summation of contributions of signal 1 and 2.

B. Measurement Setup

The schematic and photos of the measurement setup are shown in Fig. 6. Three signals are measured simultaneously by the oscilloscope: line signal of the LISN and two reference signals. Simultaneous measurements are essential to avoid losing the correlation between the signals. The reference signals are measured by the magnetic near-field probes. The probing locations are selected manually such that each probe is coupled predominantly to just one source (PFC or H-bridge). The quality of the reference signals is controlled by calculating the coherence between them, a low value indicates small leakage between the reference channels. The measurement setup is placed in a chamber to reduce the environmental noise. In

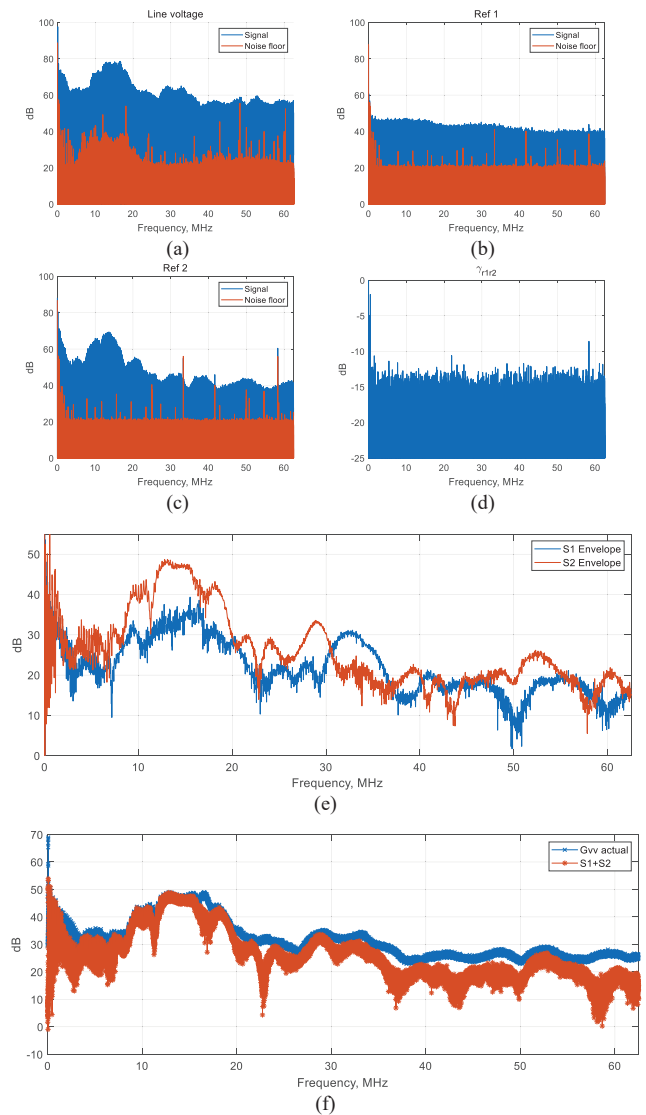


Fig. 10. Measurement results at 125 MS/s for the 1600W PSU. (a) Line signal vs. noise floor. (b) Reference 1 vs. noise floor. (c) Reference 2 vs. noise floor. (d) Coherence between reference 1 and 2. (e) Calculated contribution envelopes of signal 1 and 2. (f) Comparison between the power density of line signal and summation of contributions of signal 1 and 2.

addition, high pass filters are added to all three channels to avoid overloading of the oscilloscope by strong low-frequency components of the signals. A network of power resistors is used as an equivalent load of the PSUs during the test.

C. Measurement Results and Analysis

Before the signal separation process, the spectra of three signals are checked at low frequencies first (up to 1 MHz), to make sure the locations of the probes are optimized well. The low frequency spectra of the signals for the 900W PSU are shown in Fig. 7. It demonstrates that the line signal contains two major signals which are captured in the reference channels as well. The PFC signals is marked by the red block, and the H-bridge signal is marked by the green block. The reference 1

signal contains predominantly the PFC signal while the level of the H-bridge signal in that channel is much lower, and the reference 2 signal mainly contains the H-bridge signal. The coherence between reference 1 and 2 is plotted in Fig. 8 (a). The coherence value can be used to assess the leakage (unwanted coupling) between the two references. In this case, acceptable decoupling is achieved below 7 MHz (coherence is below -5 dB), and good decoupling is shown from 7MHz to 40 MHz (coherence is below -10 dB). The quality of the coherence-based signal separation can be assessed by comparing the spectra at low frequencies where the signals are separable in the frequency domain. In Fig. 8 (b), the separated power densities (according to (11) and (12)) of signals 1 and 2 are shown. By taking the sum of them it is possible to reproduce the total line voltage power density with an accuracy of not worse than 5 dB above 100 kHz (Fig. 8(c), purple line). Also, the contributions of the two sources are clearly separated in the spectra S_1 and S_2 – the PFC contribution is dominant in the spectrum S_1 and the H-bridge contribution is dominant in the spectrum S_2 .

Afterwards, the signal separation method is applied to the two PSU at higher frequencies. For both PSUs, the reference 1 channel measures the PFC signal and reference 2 channel measures the H-bridge signal.

Fig. 9 shows the measurement results with the sampling rate of 125 MS/s on the 900W PSU. The comparison between the signals and noise floors (measured with the DUT turned off) of three channels are shown in Fig. 9 (a), (b), (c), separately. The signal-to-noise ratios are good for all three channels (at least 15 dB). The coherence between the reference signals is shown in Fig. 9 (d) and the calculated power spectral contribution envelopes of the signals 1 and 2 are shown in Fig. 9 (e). The figure demonstrates that below 26 MHz signal 1 dominates, at higher frequencies signal 1 and signal 2 have similar contributions. The comparison between the actual power spectral density of the line signal and the summation of calculated power contributions is shown in Fig. 9 (f). The difference is less than 6dB for the entire frequency range, which demonstrates successful estimation of the contributions of two major signals.

Similarly, the measurement results for the 1600W PSU are shown in Fig. 10. From the signal separation results, it can be noticed that the contributions of PFC and H-bridge sources to the conducted emissions for the two PSU models are qualitatively different: below 30 MHz the H-bridge signal dominates for the 1600W PSU, while the PFC signal dominates

for the 900W PSU. Overall, the proposed signal separation method is validated through the measurements.

IV. CONCLUSION

In this paper, a signal separation method based on coherence function is presented, which is validated on two commercial PSUs. The conducted emission, as the mixed signal, is measured at the LISN port, while two reference signals are measured by the near-field probes. By calculating the coherence between the mixed and the reference signals, the contributions of each signal could be obtained. The summation of calculated power densities of the two signals shows good agreement with actual power density of the mixed signal. Measurement of the signal contributions could be helpful for engineers to determine the dominant sources and mitigate the emissions more efficiently in a broad frequency range.

ACKNOWLEDGMENT

This paper is based upon work supported partially by the National Science Foundation under Grant No. IIP-1916535.

REFERENCES

- [1] Y. Wang, S. Bai, X. Guo, S. Jin, Y. Zhang, J. Eriksson, L. Qu, J. Huang and J. Fan, "Conducted-emission modeling for a switched-mode power supply (SMPS)," *2015 IEEE Symposium on Electromagnetic Compatibility and Signal Integrity*, 2015, pp. 314-319.
- [2] B. Zheng and J. He, "Conducted emission analysis and suppression design of a DC/DC semi-isolated power supply," *2017 IEEE International Symposium on Electromagnetic Compatibility & Signal/Power Integrity (EMCSI)*, 2017, pp. 383-387.
- [3] V. V. Bodake, S. Gupta, S. Bhat and V. R. D., "Modelling and Simulation of Conducted Emission For Electronic Control Module," *2019 IEEE 5th Global Electromagnetic Compatibility Conference (GEMCCON)*, 2019, pp. 1-4.
- [4] M. A. Rafiq, M. Amin and J. Yousaf, "Effect of shielding, grounding, EMI filters & ferrite beads on radiated & conducted emissions," *2013 6th International Conference on Recent Advances in Space Technologies (RAST)*, 2013, pp. 583-588.
- [5] C. -H. Lee, D. -B. Lin and H. -P. Lin, "A New Design of AC Voltage Probe for EMI Conducted Emission Measurement," *2020 International Workshop on Electromagnetics: Applications and Student Innovation Competition (iWEM)*, 2020, pp. 1-4.
- [6] K. Li, K. See and R. M. Sooriya Bandara, "Impact Analysis of Conducted Emission Measurement Without LISN," in *IEEE Transactions on Electromagnetic Compatibility*, vol. 58, no. 3, pp. 776-783, June 2016.
- [7] J. S. Bendat, A. G. Piersol, *Random Data*, New York: Wiley, 2010, pp. 135.